

A Dual-Port Single-Dipole MIMO Antenna Pair Based on Selective Modal Excitation for 5G Metal-Rimmed Terminals

LONGYUE QU¹, (Member, IEEE), AND HAIYAN PIAO²

¹School of Electronics and Information Engineering, Harbin Institute of Technology, Shenzhen 518055, China

²Hanyang Antenna Design Company Ltd., Shenzhen 518100, China

Corresponding author: Longyue Qu (rioinkorea@gmail.com)

ABSTRACT This study presents a dual-port single-dipole MIMO antenna pair, which is accomplished by selectively exciting the dominant dipole-type current mode and the second higher current mode of a single suspended metal strip. A magnetic coupling method based on a feeding loop is implemented at the current maximum portion of the dominant mode of the suspended metal strip, such that the suspended metal strip operates as a half-wavelength dipole radiator. An electrical coupling method based on a feeding capacitor, otherwise, excites the wavelength dipole mode of the suspended metal strip, and this higher mode resonance is further controlled by a tuning capacitor. In this way, the suspended metal strip involves a dual-port MIMO antenna pair, and both antennas operate as dipole-type radiators while having high port-to-port isolation because of the modal orthogonality. Therefore, the operation mechanism of the proposed technique is straightforward, and the implementation is simple, free of any additional decoupling components or a complex excitation network. This feature makes the proposed technique an attractive solution in metal-rimmed terminals for 5G applications, so 4×4 MIMO antennas operating at the N78 band were constructed and verified in both simulation and measurement.

INDEX TERMS Dual-port single-dipole, MIMO, magnetic coupling, electric coupling, metal-rimmed terminals, 5G.

I. INTRODUCTION

Multiple-input multiple-output (MIMO) technology has been widely adopted in 4G LTE and 5G applications; by scaling up the number of antenna elements, channel capacity can be dramatically increased [1], [2]. Due to the wireless traffic from the proliferation of user numbers and the explosion of more powerful cellular devices, 5G is now in explosive expansion to satisfy the desperate demand for ultra-fast speeds, low latency, and outstanding reliability. For this reason, a large-scale antenna array must be deployed in current and future 5G terminals.

Nevertheless, decoupling and decorrelation of MIMO antenna systems have always been challenging works, and this is especially true in terminal devices due to close antenna

arrangement, causing strong mutual coupling, severe interference, and low radiation efficiency. Therefore, solutions to the integration of large-scale antenna elements in crowded terminals are of great interest. In the literature, various decoupling and decorrelating techniques have been proposed to decrease the distance between antenna elements [3]–[8] and even to realize spatial reuse [9]–[18]. The adopted methods include neutralization lines, decoupling networks, additional elements, pattern or diversity control, etc.

In addition, metal rims have been popularly used in various terminals, such as smartphones and tablets, due to market demand and customer preference. Under these circumstances, the introduction of large-scale MIMO antenna elements in the sub-6 GHz band is facing great challenges, and the above-mentioned methods may be inapplicable. Recent studies have presented several integration methods of 5G MIMO antennas for metal-rimmed terminals [19]–[24].

The associate editor coordinating the review of this manuscript and approving it for publication was Davide Ramaccia¹.

TABLE 1. Comparisons with the state of the art on metal-rimmed MIMO antennas.

Ref.	Decoupling method	Implementation method	-6dB impedance bandwidth	Isolation	Measured efficiency	Complexity
[19]	Neutralization line	8.5 mm separation between two antenna elements	Dual-band (>200 MHz, >400 MHz)	>10 dB	>44%	Large clearance and large distance
[20]	Orthogonal monopole/dipole mode	Shared radiator with parasitic slots	1700 MHz	>21 dB	>31.6%	Complex feeding method and components
[21]	Orthogonal modes	Shared slot	>200 MHz	>24 dB	>35%	Complex matching network, difficult installment, and narrow bandwidth
[22]	Orthogonal modes	Integrated loop and slot	>200 MHz	>19 dB	>59%	Difficult installation and narrow bandwidth
[23]	Connecting line	Edge-to-edge slots	>1700 MHz	>10 dB	>52%	Difficult fabrication and low isolation
[24]	Mixed method	Edge-to-edge slots	>1700 MHz	>10 dB	>40%	Difficult fabrication and low isolation
This work	Mode control	Shared dipole	>500 MHz	>16 dB	>68%	Simple and new

In [19], a link line is utilized between antenna elements to enhance the isolation, but the distance is still very large. In [20] and [21], complex excitation and matching methods are necessary to excite orthogonal current modes for the purpose of self-decoupled performance, which may not be preferred in practical scenarios. The proposed methods in [21] and [22], otherwise, mainly suffer from difficult implementation and narrow bandwidth. The studies in [23], [24] combined the methods in [9], [11] so that the antenna elements are disposed of close to each other, however, the integration level is not high enough and the fabrication is not easy to achieve. A comparison table with the state of the art is concluded in Table 1 to further address the novelty of the proposed work.

Therefore, this study focuses on discovering a simple and straightforward MIMO pair solution with enhanced spatial utilization ratio and integration level, intended for metal-rimmed terminals. The proposed dual-port single-dipole MIMO antenna pair consists of just one suspended metal rim, whose dominant dipole-type current mode and higher current mode are selectively excited and simultaneously operating at the N78 band. In this way, the suspended metal rim operates as a dual-port single-dipole MIMO antenna pair, even though the two antennas share the same structure and the antenna ports are extremely close to each other. The dominant contribution of the proposed technique lies in its more straightforward mechanism and much easier implementation method when compared to previously reported spatial-reused MIMO antenna pair solutions. Both simulation and measurement were conducted to demonstrate the practicality of the proposed technique for 5G terminals.

II. DUAL-PORT SINGLE-DIPOLE MIMO ANTENNA PAIR

A. MIMO ANTENNA CONFIGURATION

The configurations of the proposed dual-port single-dipole MIMO antenna pair are depicted in Fig. 1, where a

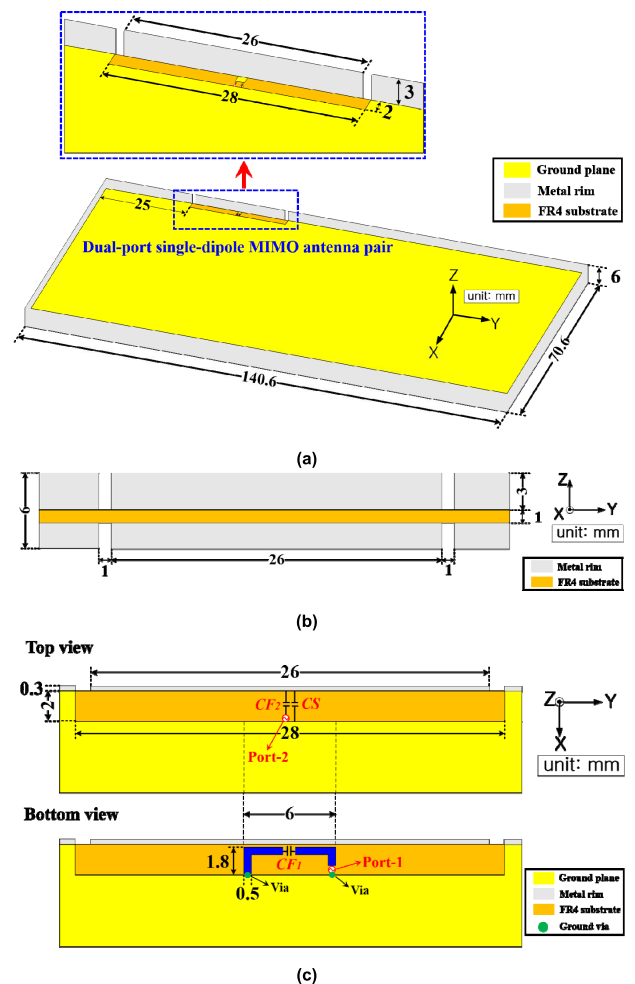


FIGURE 1. Configurations of the proposed MIMO antenna pair: (a) perspective view, (b) side view of the metal rim, and (c) zoomed view of the antenna pair.

140 mm × 70 mm ground plane, surrounded by metal strips, is used to model the metal-rimmed smartphone

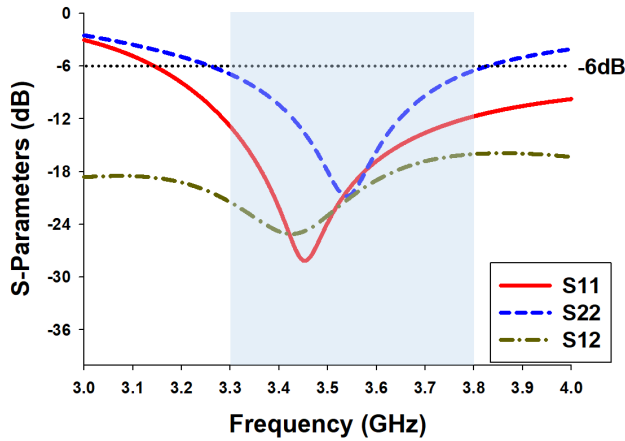


FIGURE 2. Simulated S-parameters of the proposed MIMO antenna pair.

scenario. The height and the thickness of the metal strips are 6 mm and 0.3 mm, respectively. Meanwhile, the ground plane is fabricated on a 1-mm-thick FR4 substrate ($\epsilon_r = 4.4$, $\tan \delta = 0.02$). The proposed MIMO antenna pair is constructed by utilizing a 26-mm-long suspended metal strip and a 2 mm \times 28 mm ground clearance. It is seen that the suspended metal strip is isolated from other metal strips by two gaps or cuts. Herein, the dominant current mode and the higher mode of the suspended metal strip are excited by Port 1 and Port 2, respectively.

For Antenna-1, a feeding loop with a feeding capacitor CF_1 is adopted at the center of the ground clearance and printed at the bottom side of the ground plane. The feeding loop is connected to a voltage source at one end and is grounded through a ground via at the other end. The overall dimension of the feeding loop is 1.8 mm \times 6 mm \times 1 mm. In this way, the feeding loop operates as a magnetic coupler to the dominant mode of the suspended metal strip, and the impedance characteristic can be conveniently controlled by adjusting the value of CF_1 . Meanwhile, the electrical length of the suspended metal strip directly determines the resonant frequency of Antenna-1.

For Antenna-2, a feeding capacitor CF_2 is firstly used for electric excitation of this higher mode resonance and control of the input impedance. A shunt tuning capacitor CS is then loaded between the suspended metal strip and the ground plane at the center of the ground clearance, responsible for resonance control of the higher mode of the suspended metal rim for N78 operation. Both CF_2 and CS are mounted at the top side of the ground plane, occupying a minimal area of 1 mm \times 2 mm. Accordingly, the proposed selective excitation technique ensures simultaneous exploiting of two modal resonances of a shared radiating structure by merely utilizing lumped elements, thereby accomplishing a dual-port single-element MIMO antenna pair. It is noted that the optimized values of CF_1 , CF_2 , and CS in the simulation are 0.25 pF, 1 pF, and 0.85 pF, respectively.

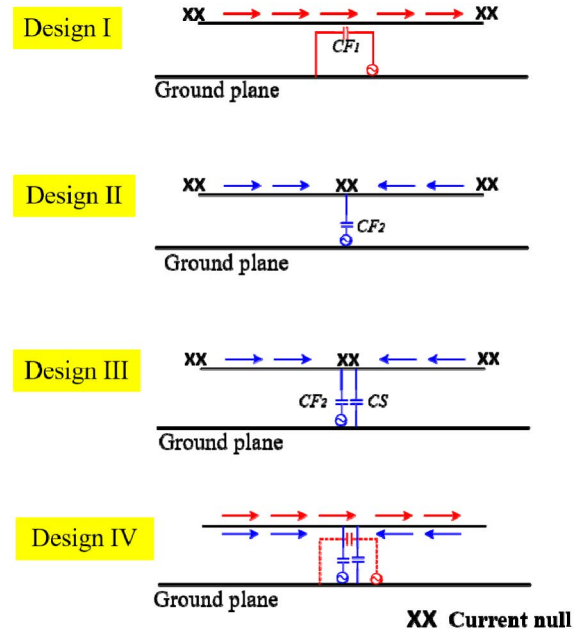


FIGURE 3. The design process of the proposed dual-port single-dipole MIMO antenna pair.

B. SIMULATION RESULTS AND OPERATION MECHANISM

The simulated scattering parameters (S-parameters) of the proposed MIMO antenna pair are presented in Fig. 2, where the MIMO antennas can produce broadband impedance bandwidths (above 500 MHz) that fully cover the N78 band. Meanwhile, it can be observed that the dominant mode resonance (Antenna-1) can produce a much wider impedance bandwidth than the higher mode resonance (Antenna-2). Furthermore, high isolation property over 16 dB in the overall frequency band can be confirmed from the S_{12} curve, indicating the feasibility of the proposed dual-port single-element MIMO antenna solution.

C. DESIGN PROCEDURE AND OPERATION MECHANISM

The design process of the proposed dual-port single-dipole MIMO antenna pair is demonstrated here to further explain its working principle, as seen in Fig. 3.

- In Design I, the dominant dipole-type mode of the suspended metal strip is presented, and a magnetic feeding method (i.e., the feeding loop) is adopted at the current maximum portion of the suspended metal strip to excite this dominant mode. It is known that the dominant dipole mode resonance is dependent on the length of the suspended metal strip, and its input impedance can be simply adjusted by controlling the value of CF_1 . In this way, Antenna-1 is constructed.
- In Design II, the second higher dipole mode of the suspended metal strip is shown, and an electric coupling method is used for excitation. For this purpose, a feeding capacitor CF_2 is simply adopted at the electric field maximum portion, i.e., at the center of the suspended metal strip. It is noted that the same metal strip in Design I is used for the design

of Antenna-2. Since the dominant mode of the metal strip is operating at its half-wavelength at the target frequency, the initial resonance of the second higher mode (Antenna-2) would be about two times higher than the target frequency.

- c. Accordingly, in Design III, a shunt capacitor CS is further loaded at the center of the suspended metal strip to lower down the higher mode resonance without affecting the dominant mode resonance, such that both modes are operating at the same frequency band for N78 applications. As a result, Antenna-2 is constructed.
- d. Design IV presents the final stage of integrating Design I and Design III. To realize structural compatibility, the feeding structure of Antenna-1 and that of Antenna-2 are allocated at the top side and bottom side of the ground plane, respectively. Though the feeding structures are located at the same position and overlapping each other, their field distributions are totally different, thus having immunity from one to another. Finally, both the dominant mode resonance and the higher mode resonance are independently controlled and selectively excited, forming a dual-port single-element MIMO antenna pair.

Further observation is discussed in Fig. 4. For Antenna-1 only, the variation of CF_1 dominantly modifies the impedance matching while barely affecting its resonance, as can be confirmed in Fig. 4(a), and this is the case in Design I. For Antenna-2 only, CF_2 is used for antenna feeding, and the antenna becomes overcoupled with increased CF_2 , deteriorating the impedance matching, as shown in Fig. 4(b). Meanwhile, CF_2 also behaves as a capacitive load and affects the antenna resonance, and this can be observed from the fact that the antenna resonance lowers down from 5.5 GHz to 4.2 GHz as CF_2 increases from 0.25 pF to 1 pF. Moreover, it is verified that the initial resonance of the second dipole mode (Antenna-2) is much higher than that of the dominant dipole mode (Antenna-1). This is the case in Design II without the shunt tuning capacitor CS . By loading the shunt tuning capacitor CS , the antenna resonance is well controlled and further decreased, as shown in Fig. 4(c), and this is the case in Design III.

To better understand the operation mechanism of the proposed technique, the simulated surface current distributions over the suspended metal strip are plotted at 3.5 GHz (see Fig. 5). It is noted that the surface current distributions are obtained when one port is excited while the other is terminated.

In Fig. 5(a), Port 1 is excited, and the current flows over the suspended metal strip are in the same direction, having two current nulls at its open ends and current maximums at its center portion. Accordingly, Antenna-1 is operating as a half-wavelength dipole-type resonator. In Fig. 5(b), Port 2 is excited, and the current directions over the suspended metal strip are against each other, having three current nulls at its two open ends and center portion. This indicates that Antenna-2 operates as a one-wavelength

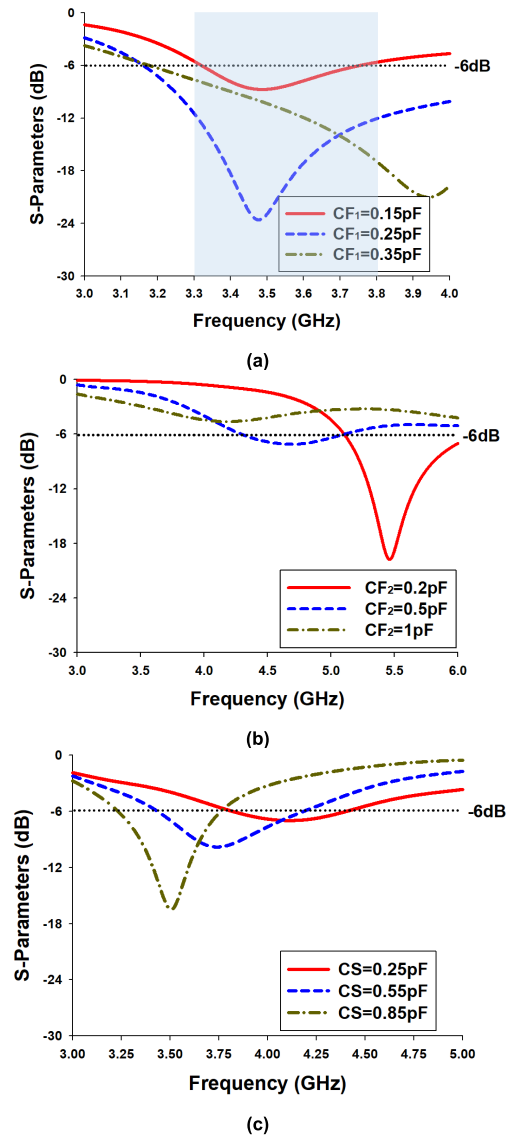


FIGURE 4. Simulated reflection coefficients: (a) for Antenna-1 only (i.e., Design I), (b) Antenna-2 only without CS (i.e., Design II), and (c) Antenna-2 only with CS (i.e., Design III).

dipole-type resonator, whose resonant frequency is decreased by the loaded capacitors (CF_2 and CS). Therefore, it can be concluded that the proposed technique is a novel dual-port single-dipole MIMO antenna pair that is accomplished by utilizing two orthogonal current modes of the shared suspended metal strip. Furthermore, it is clearly seen that Antenna-1 produced in-phase current distributions while Antenna-2 produced out-of-phase current distributions. This fact determines that Antenna-1 is a better radiator than Antenna-2, and explains the bandwidth difference between the two antenna ports.

III. DEMONSTRATION OF 4×4 MIMO ANTENNA ARRAY

A. ANTENNA CONFIGURATION

Based on the previous discussion, a large-scale MIMO antenna system can be accomplished by simply duplicating

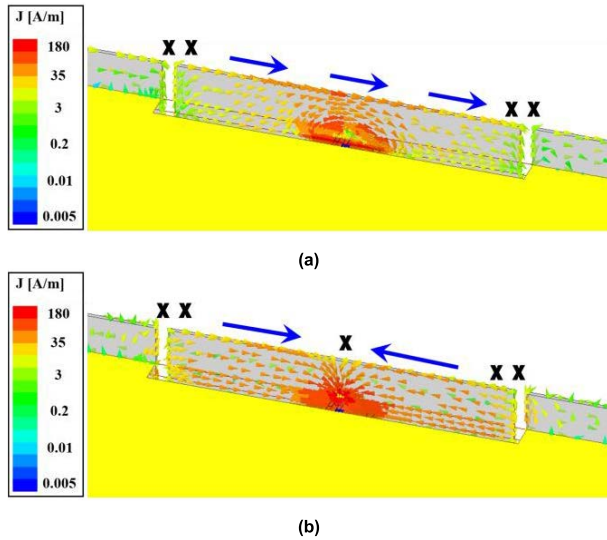


FIGURE 5. Simulated surface current distributions at 3.5 GHz: (a) excitation of Port 1 and (b) excitation of Port 2.

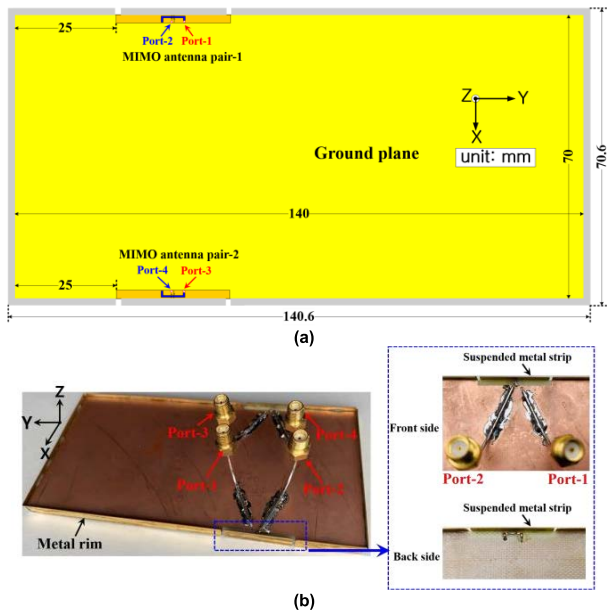


FIGURE 6. 4 × 4 MIMO antennas for 5G applications: (a) simulation model, and (b) fabrication prototype.

the aforementioned antenna pair solution, intended for current and future terminal devices. For this purpose, a 4 × 4 MIMO antenna system is established as a case study (see Fig. 6). In industry, the 3G/4G antenna systems, usually imposed at the upper and lower ends of a smartphone, will coexist with the 5G systems for a long time. Therefore, the proposed 5G antennas should be allocated at the two sides of the ground plane, as shown in Fig. 6(a). Besides, the prototype of the fabrication is pictured in Fig. 6(b).

B. SIMULATION AND MEASUREMENT

In this subsection, both the simulated and measured results of the proposed 4 × 4 MIMO antennas are demonstrated to

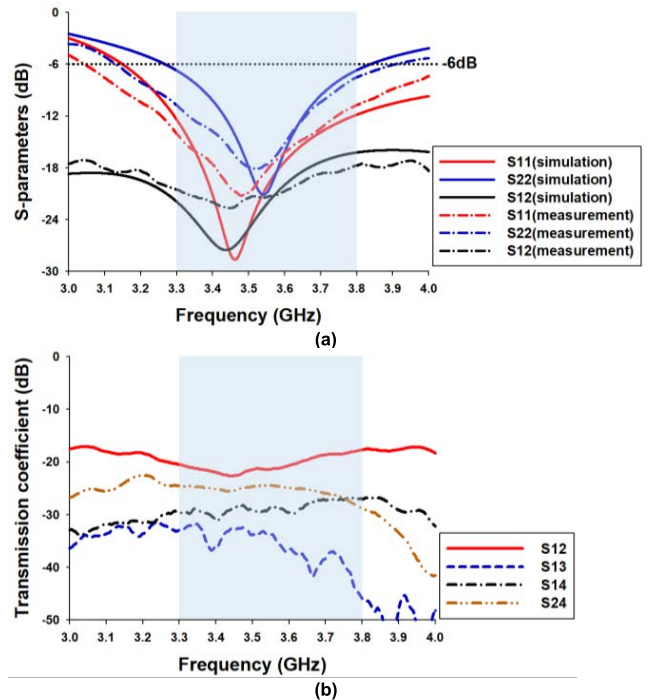


FIGURE 7. Simulated and measured results: (a) S-parameters, and (b) measured transmission coefficients.

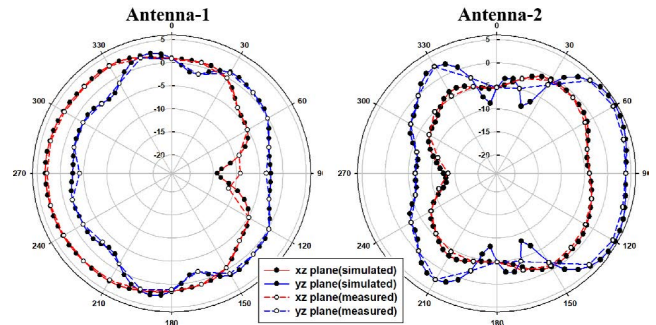


FIGURE 8. Simulated and measured radiation patterns at 3.5 GHz.

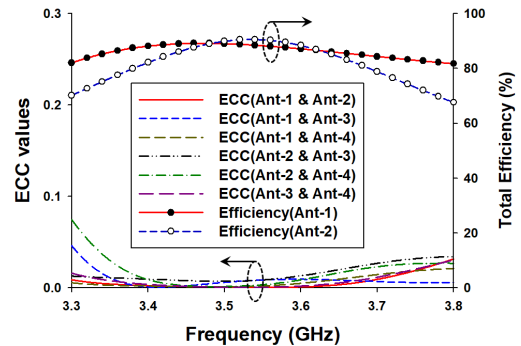


FIGURE 9. Measured ECC values and total efficiencies of the fabricated antennas.

verify the performance of the proposed technique. It is noted that the fabrication was tested using a network analyzer and measured in a 6 m × 3 m × 3 m three-dimensional (3D) CTIA OTA anechoic chamber. Besides, the used capacitor values

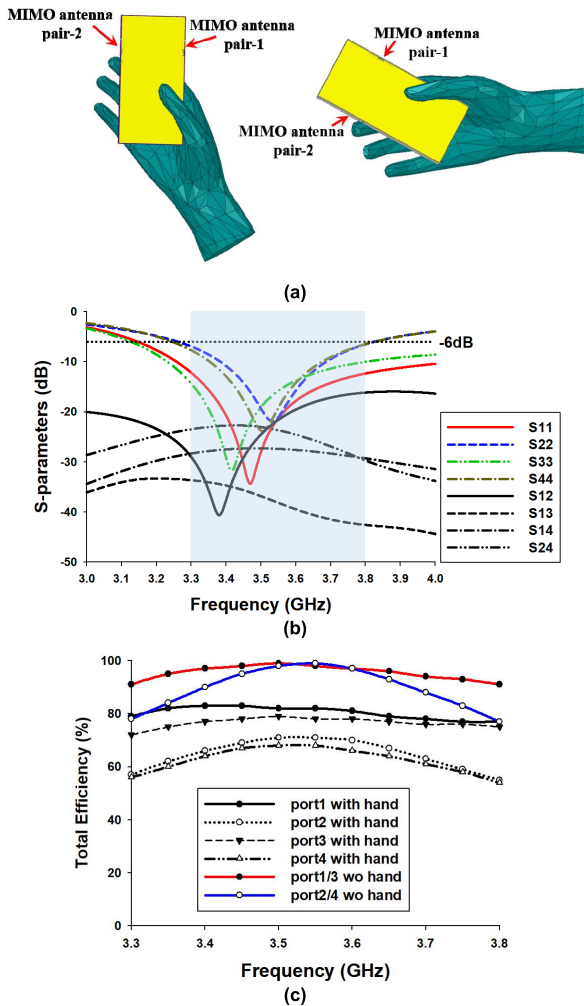


FIGURE 10. Hand effect in simulation: (a) simulation model, (b) S-parameters, and (c) total efficiencies.

of CF_1 , CF_2 , and CS in measurement were 0.3 pF, 1 pF, and 0.8 pF, respectively.

First of all, the simulated and measured S-parameters are given in Fig. 7. As can be observed in Fig. 7(a), the S_{11} and S_{22} curves can fully cover the 3.5 GHz frequency band, and the mutual coupling (S_{12}) is lower than -18 dB in measurement. The measured results are consistent with the simulated ones only with a minor discrepancy, which may be attributed to the fabrication error. As can be observed from the measured transmission coefficients in Fig. 7(b), the isolation between any two antenna elements is above 18 dB, indicating their feasibility in industrial scenarios.

Additionally, Fig. 8 displays the produced far-field radiation patterns at 3.5 GHz in the xz -, yz -, and xy -planes. It is seen that the proposed dual-port single-dipole MIMO antenna pair produced approximately complementary radiation patterns with maximum gains directed against each other, which is an attractive feature for signal reception. Herein, correlation is an important figure-of-merit to assess the diversity performance of MIMO antennas, which can be

derived from the vector properties (amplitude, phase, and polarization) of the complex far-field radiation patterns [25]. Therefore, envelope correlation coefficient (ECC) ρ_e are calculated and plotted in Fig. 9, where the values are all below 0.1, which is far lower than the acceptable criterion ($\rho_e < 0.5$) in mobile communications. Besides, the measured total efficiencies are also plotted in Fig. 9, and it can be seen that both antennas can produce high radiation efficiencies over 68% within the overall operation band. Accordingly, the proposed dual-port single-dipole MIMO antenna solution is proven to have superiority on high integration, high isolation, as well as excellent radiation performance and diversity performance, making it feasible for 5G applications in current and future terminal devices.

For terminal devices, the user's hand effect is an important factor to consider. Therefore, the radiation performance of the proposed MIMO antennas under the right-hand mode is investigated in the simulation, as shown in Fig. 10(a). As can be observed from the S-parameters in Fig. 10(b), the reflection coefficient produced by each port barely changed with only a slight modification, which can still cover the N78 band. The isolation between every two ports is higher than 16 dB. In Fig. 10(c), the simulated total efficiencies of Port 1 (Port 3) and Port 2 (Port 4) in free space (without hand) are above 91% and 78%, respectively. With the hand effect, the efficiencies produced by each port decreased by about 20%. Meanwhile, it can be seen that the MIMO antenna pair 2 (Port 3 and Port 4) has a slightly larger effect than the MIMO antenna pair 1 (Port 1 and Port 2). This is attributed to the fact that the hand fingers are closer to the MIMO antenna pair 2, resulting in a greater attenuation from the user's hand. Since both two antennas pairs are located at the upper side of the ground plane, they are not directly touched by the user's fingers or palm so that the effect on the S-parameters and efficiency attenuation is limited.

IV. CONCLUSION

This study presents a novel dual-port single-dipole MIMO antenna pair, which is a simple and straightforward solution especially suitable for metal-rimmed terminals. One suspended metal strip is tactfully utilized, simultaneously operating as a half-wavelength dipole-type radiator and a wavelength dipole-type radiator. Herein, a selectively modal excitation method is proposed so that the feeding loop can selectively excite the half-wavelength dipole-type mode based on magnetic coupling and the feeding capacitor can selectively excite the wavelength dipole-type mode based on electric coupling. In this way, the suspended metal strip operates as a dual-port single-element MIMO antenna pair with self-decoupling and decorrelation properties. Two sets of the proposed MIMO antenna pair, constructing 4×4 MIMO antennas, were fabricated and measured. In measurement, broadband bandwidths over 500 MHz were produced. Meanwhile, high isolation above 18 dB and low ECC below 0.1 are also confirmed, indicating their feasibility in industrial scenarios.

REFERENCES

- [1] E. Björnson, E. G. Larsson, and T. L. Marzetta, "Massive MIMO: Ten myths and one critical question," *IEEE Commun. Mag.*, vol. 54, no. 2, pp. 114–123, Feb. 2016.
- [2] A. Al-Wahhamy, H. Al-Rizzo, and N. E. Buris, "Efficient evaluation of massive MIMO channel capacity," *IEEE Syst. J.*, vol. 14, no. 1, pp. 614–620, Mar. 2020.
- [3] K.-L. Wong, C.-Y. Tsai, and J.-Y. Lu, "Two asymmetrically mirrored gap-coupled loop antennas as a compact building block for eight-antenna MIMO array in the future smartphone," *IEEE Trans. Antennas Propag.*, vol. 65, no. 4, pp. 1765–1778, Apr. 2017.
- [4] Z. Ren, A. Zhao, and S. Wu, "MIMO antenna with compact decoupled antenna pairs for 5G mobile terminals," *IEEE Antennas Wireless Propag. Lett.*, vol. 18, no. 7, pp. 1367–1371, Jul. 2019.
- [5] C. Deng, D. Liu, and X. Lv, "Tightly arranged four-element MIMO antennas for 5G mobile terminals," *IEEE Trans. Antennas Propag.*, vol. 67, no. 10, pp. 6353–6361, Oct. 2019.
- [6] H. Piao, Y. Jin, and L. Qu, "Isolated ground-radiation antenna with inherent decoupling effect and its applications in 5G MIMO antenna array," *IEEE Access*, vol. 8, pp. 139892–139902, 2020.
- [7] Z. Xu and C. Deng, "High-isolated MIMO antenna design based on pattern diversity for 5G mobile terminals," *IEEE Antennas Wireless Propag. Lett.*, vol. 19, no. 3, pp. 467–471, Mar. 2020.
- [8] H. Piao, Y. Jin, Y. Xu, and L. Qu, "MIMO ground-radiation antennas using a novel closed-decoupling-loop for 5G applications," *IEEE Access*, vol. 8, pp. 142714–142724, 2020.
- [9] S.-W. Su, C.-T. Lee, and S.-C. Chen, "Very-low-profile, tri-band, two-antenna system for WLAN notebook computers," *IEEE Antennas Wireless Propag. Lett.*, vol. 17, no. 9, pp. 1626–1629, Sep. 2018.
- [10] N. O. Parchin, Y. I. A. Al-Yasir, A. H. Ali, I. Elfegani, J. M. Noras, J. Rodriguez, and R. A. Abd-Alhameed, "Eight-element dual-polarized MIMO slot antenna system for 5G smartphone applications," *IEEE Access*, vol. 7, pp. 15612–15622, 2019.
- [11] K.-L. Wong, B.-W. Lin, and S.-E. Lin, "High-isolation conjoined loop multi-input multi-output antennas for the fifth-generation tablet device," *Microw. Opt. Technol. Lett.*, vol. 61, no. 1, pp. 111–119, Jan. 2019.
- [12] H. Xu, S. Gao, H. Zhou, H. Wang, and Y. Cheng, "A highly integrated MIMO antenna unit: Differential/common mode design," *IEEE Trans. Antennas Propag.*, vol. 67, no. 11, pp. 6724–6734, Nov. 2019.
- [13] H. Piao, Y. Jin, and L. Qu, "A compact and straightforward self-decoupled MIMO antenna system for 5G applications," *IEEE Access*, vol. 8, pp. 129236–129245, 2020.
- [14] C.-Z. Han, L. Xiao, Z. Chen, and T. Yuan, "Co-located self-neutralized handset antenna pairs with complementary radiation patterns for 5G MIMO applications," *IEEE Access*, vol. 8, pp. 73151–73163, 2020.
- [15] L. Chang, Y. Yu, K. Wei, and H. Wang, "Orthogonally polarized dual antenna pair with high isolation and balanced high performance for 5G MIMO smartphone," *IEEE Trans. Antennas Propag.*, vol. 68, no. 5, pp. 3487–3495, May 2020.
- [16] C.-C. Wan and S.-W. Su, "Dual-feed, dipole antenna system for 2.4/5.2/5.8-GHz, tri-band WLAN laptop applications," *Prog. Electromagn. Res. C*, vol. 102, pp. 175–185, 2020.
- [17] C. Lee and S. Su, "Decoupled multi-input multi-output antennas with a common dipole for wideband 5G laptop computers," *Microw. Opt. Technol. Lett.*, vol. 63, no. 4, pp. 1286–1293, Apr. 2021.
- [18] T. Yuan, Z. Chen, T. Gu, and T. Yuan, "A wideband PIFA-pair-based MIMO antenna for 5G smartphones," *IEEE Antennas Wireless Propag. Lett.*, vol. 20, no. 3, pp. 371–375, Mar. 2021.
- [19] Y. Li, C.-Y.-D. Sim, Y. Luo, and G. Yang, "Metal-frame-integrated eight-element multiple-input multiple-output antenna array in the long term evolution bands 41/42/43 for fifth generation smartphones," *Int. J. RF Microw. Comput. Aided Eng.*, vol. 29, no. 1, Jan. 2019, Art. no. e21495.
- [20] L. Sun, Y. Li, Z. Zhang, and Z. Feng, "Wideband 5G MIMO antenna with integrated orthogonal-mode dual-antenna pairs for metal-rimmed smartphones," *IEEE Trans. Antennas Propag.*, vol. 68, no. 4, pp. 2494–2503, Apr. 2020.
- [21] L. Chang, Y. Yu, K. Wei, and H. Wang, "Polarization-orthogonal co-frequency dual antenna pair suitable for 5G MIMO smartphone with metallic bezels," *IEEE Trans. Antennas Propag.*, vol. 67, no. 8, pp. 5212–5220, Aug. 2019.
- [22] A. Ren, Y. Liu, and C.-Y.-D. Sim, "A compact building block with two shared-aperture antennas for eight-antenna MIMO array in metal-rimmed smartphone," *IEEE Trans. Antennas Propag.*, vol. 67, no. 10, pp. 6430–6438, Oct. 2019.
- [23] L. Sun, Y. Li, and Z. Zhang, "Wideband decoupling of integrated slot antenna pairs for 5G smartphones," *IEEE Trans. Antennas Propag.*, vol. 69, no. 4, pp. 2386–2391, Apr. 2021.
- [24] L. Sun, Y. Li, and Z. Zhang, "Wideband integrated quad-element MIMO antennas based on complementary antenna pairs for 5G smartphones," *IEEE Trans. Antennas Propag.*, vol. 69, no. 8, pp. 4466–4474, Aug. 2021.
- [25] R. G. Vaughan and J. B. Andersen, "Antenna diversity in mobile communications," *IEEE Trans. Veh. Technol.*, vol. VT-36, no. 4, pp. 149–172, Nov. 1987.



LONGYUE QU (Member, IEEE) received the M.S. and Ph.D. degrees in electromagnetics and microwave engineering from Hanyang University, Seoul, Republic of Korea, in 2015 and 2018, respectively. He was a Postdoctoral Researcher at Hanyang University, from September 2018 to August 2019, after which he was promoted to an Assistant Research Professor. He was a Co-Founder and the CTO of Hanyang Antenna Design Company Ltd., Shenzhen, China, from 2019 to 2022. Since 2022, he has been with the School of Electronics and Information Engineering, Harbin Institute of Technology, Shenzhen, as an Assistant Professor. He has authored more than 40 articles and more than 30 inventions. He is a reviewer of several international journals and conferences. His current research interests include antenna theory and designs, metamaterial-based antenna technology, millimeter-wave arrays, and RF circuits. He is also an Editorial Board Member of the *International Journal of Sensors, Wireless Communications and Control*. He was a recipient of the Korean Government Scholarship Award and the China Scholarship Council. His research was listed in the Top 100 National Research and Development Excellence Award, in 2015.



HAIYAN PIAO received the B.Sc. degree in communication engineering from Yanbian University, China, in 2013, and the M.Sc. degree from the Department of Microwave Engineering, Hanyang University, Seoul, South Korea, in 2017. She is currently a Senior Engineer at Hanyang Antenna Design Company Ltd., Shenzhen, China. Her research interests include antennas for MIMO, 5G communication, and the IoT devices.

...